

Design Implications for Improving an Anthropomorphic Test Device based on Human Body Simulations

Karin Brolin¹, Manuel Mendoza-Vazquez¹, Eric Song², Erwan Lecuyer², Johan Davidsson¹

Abstract To evaluate new restraint systems more advanced test tools are required. To guide the design of an Anthropomorphic Test Device (ATD) torso, simulations were performed with the LS-DYNA and RADIOSS codes using two human body models: an improved Total HUMAN Model for Safety (THUMS) version 3.0 and the HUMOS2LAB model. The baseline models were modified by removing a selection of internal organs, changing tissue stiffness and density, and/or blocking spinal joints to resemble ATD-like simplifications. Experimental setups with loading to the chest from an impactor, belts and airbag were simulated and the rib strains, mid sternal deflection and differential deflections from other assessment points on the rib cage, and thoracic effective stiffness were compared. Changing the material properties of intercostal muscles, ribs and sternum had the greatest influence on the differential deflections. Removing internal organs resulted in a global stiffness decrease of the thorax. However, it does not change the main features of the rib strain profile. If the lack of internal organs is compensated in an ATD by using stiffer rib materials, the differential deflections will decrease. There is a compromise between stiffness and mass representation in order to measure biofidelic differential chest deflections.

Keywords Anthropomorphic test device, human body model, thorax, finite element

I. INTRODUCTION

In 2000, traffic accidents resulted in severe injuries to the head and thorax more frequently than injury to other body regions [1]. In 2003, the safety effect associated with the introduction of airbags had reduced head injuries while thoracic injuries were still a major factor in accidents resulting in severe or fatal injuries [2]. In 2006, the thorax was still a dominant body region for severe and fatal injuries [3].

Anthropomorphic Test Devices (ATDs) have been used in the automotive industry since the early 1950's to evaluate and develop safety systems. The current ATDs used to evaluate frontal crashes are the Hybrid III dummy (currently used in European legislation and consumer testing) and the THOR dummy, the intended successor of the Hybrid III dummy [4]. The chest responses of these ATDs are based on a set of experimental biomechanical data which is limited due to its predominant reliance on pendulum impacts. Such pendulum impacts are far from the loading experienced by a human occupant in a modern car, fitted with restraint systems such as 3-point belts with load limiters and pretension and a variety of airbags. It has become clear that the current frontal impact dummies are not sensitive to the modern restraint systems [5]-[6], implying that improvement regarding the thoracic biofidelity is needed. Using ATDs devoid of human thoracic responses may lead to sub-optimised restraint systems and stagnation in the risk reduction of thoracic injuries. This is in line with the PRISM study [2] that found thoracic injuries to be present in less severe accidents in relation to car crash testing, than expected. This was attributed in part to the limitations of the Hybrid III dummy. A similar conclusion was drawn when EuroNCAP ratings were compared to real world safety performance [7].

These findings indicated the need to further study the thorax region and improve the existing ATDs to reliably predict the human impact response correlating to injuries seen in real life accidents. Human volunteer, human cadaver or animal testing can be performed to increase the understanding of thoracic responses to loading. However, it is very complex and expensive, if at all possible, to evaluate the impact of different simplifications in the ATD's design using the above mentioned methods. An alternative strategy is to use digital human body models to simulate a variety of impact conditions making it possible to estimate the influence of ATD-like simplifications on the thoracic response in terms of stiffness, strain and displacements, for example,

¹K Brolin is Associate Prof. at Chalmers University of Technology in Sweden (+46 31 7721509, karin.brolin@chalmers.se). ¹M Mendoza-Vazquez is graduate student at Chalmers University of Technology in Sweden. ²E Song and E Lecuyer are research engineers at LAB Peugeot Citroën Renault in France. ¹J Davidsson is Assistant Prof. at Chalmers University of Technology in Sweden.

which is the approach adopted for this study. The aim is to estimate how simplifications to the human thorax, making it more similar to an ATD, will influence the responses in loading conditions representative of modern restraint systems and give recommendations for future ATD design improvement.

II. METHODS

Simulations were performed with the Finite Element (FE) codes LS-DYNA version 970 [8] and RADIOSS [9], using two 50th percentile male human body models: the Total HUMAN Model for Safety (THUMS) version 3.0 [10] and the HUMOS2LAB model [11]. The models have been modified as described below to improve biofidelity of the thorax and are hereafter defined as baseline models. Then, as described in the subsection Model modifications, the baseline models were modified by removing internal organs, changing the tissue stiffness, changing the mass distribution and blocking spinal joints. The baseline and modified models were used to simulate several experimental setups as described in the subsection Simulations. Pre and post processing were performed with LS-PREPOST (LSTC Inc.), Visual-Environment (ESI Inc.), MatLab (The Mathworks Inc.), Altair Hyperworks (Altair Engineering Inc.), and Oasys Primer (ARUP Inc.).

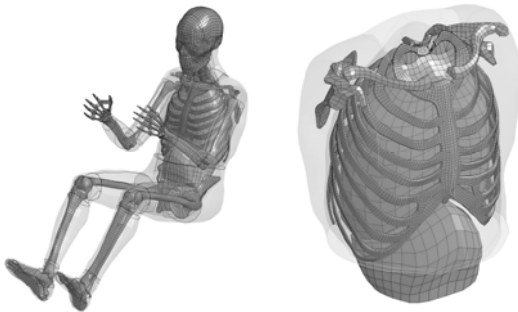


Fig. 1. Overall view and the thoracic part of the THUMS baseline model.

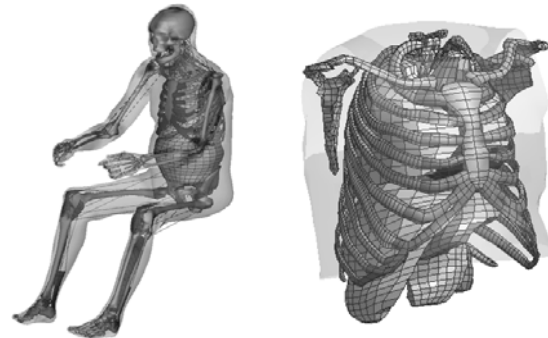


Fig. 2. Overall view of HUMOS2LAB and the thoracic part of the HUMOS2LAB baseline model.

THUMS baseline model

THUMS version 3.0 was developed by Toyota Motor Corporation [12]-[13] in the LS-DYNA FE code. In the thorax, the ribs were modelled with shell elements for the cortical and solid elements for the trabecular bone. The cartilage between the sternum and the ribs was also represented by solid elements. The internal organs inside the rib cage were represented by two volumes meshed with solid elements and the abdominal organs with one volume of solid elements. The costovertebral ligaments were modelled with spring elements. Different versions of the THUMS thoracic cage have been validated in the past, most of which have been validated against pendulum impacts such as those reported in [14]-[15] and others against table top tests [16] and whole-body kinematics [17]. Changes to the thorax, including refined mesh of the rib cage, skin and intercostal muscles, were implemented to improve the robustness and numerical stability [18], see Figure 1. In this study, the material properties used in the thoracic flesh and the lungs were adjusted. The flesh was updated according to the material properties published in [19]. The material for the lungs was modified by decreasing its stiffness according to Post Mortem Human Subject (PMHS) experiments [20]. The model resulting from these modifications will hereafter be referred to as the THUMS baseline model. The THUMS baseline model's thoracic response is compared in [21] to those of PMHSs in experimental pendulum impacts according to [22], table top tests by [20], [23]-[24] and sled tests by [25].

HUMOS2LAB baseline model

The HUMOS2LAB model is an improved version of the HUMOS model which is a full human body finite element model developed by a consortium of universities, research institutes and car manufacturers [26]. Its mesh was constructed based on the geometry of a single subject whose mass, stature and seated height were close to an average sized European male. However, the subject presented a more massive torso and less massive lower extremities, typical for an aged person. The Laboratory of Accidentology and Biomechanics (LAB) was in charge of modeling the shoulder and the thorax in the RADIOSS™ FE code during the first phase of the HUMOS model development. The HUMOS model was further updated with respect to new biomechanical data available in the later stages of its development [11]. Regarding the thorax part of the HUMOS model, the cortical bone of the ribs and the sternum was represented by shell elements, and the trabecular bone by solid

elements. The cartilage between the sternum and the ribs was represented by solid elements as was the muscles and internal organs, such as the heart, lungs, stomach and liver. Elasto-plastic material law was used to model the cortical bone, elastic material law for the trabecular bone and cartilage, and Boltzman material law was used for the internal organs and muscles. The vertebrae were considered as rigid bodies and the connections between them were modelled with general springs, which is the same method used for the connections between the ribs and the vertebrae.

A number of modifications were made to the HUMOS model at the LAB. The objective was to make the model representative of the response of a human thorax, not only in terms of global responses but also in terms of local responses, such as the strain profiles and rib fractures. Hereafter, the modified model will be referred to as the HUMOS2LAB baseline model. The HUMOS2LAB baseline model was validated in [27]-[28]. Overall, the HUMOS2LAB model has proved to be consistent with the main features of current cadaver test data available at LAB and can be considered as representative of the response of a human thorax.

Model modifications

The baseline models were modified to create seven ATD-like models, and five models into which different thoracic tissues were given softer material properties, see Table I. ATD1 and ATD6 represent the THOR dummy in which the mass of the internal organs are distributed on other structures and lacking costovertebral joint motion. Furthermore, ATD6 implements the stiffer rib material compared to human bone. The other ATD-like modifications represent individual features of the THOR dummy and ATD2 comprises only the stiff rib material. The THOR dummy has longer ribs and shorter cartilage compared to humans, as implemented in ATD3. In ATD4 the upper and lower part of the sternum was decoupled and the stiffness of the first rib was increased to represent the THOR sternum and bib design. The internal organs’ of the ATD5 has negligible inertia effects while the internal organ stiffness is intact. The THOR clavicle has a horizontal orientation which was implemented by changing the angle of the clavicle contact surface in ATD7. To present a comparison, a 50% stiffness reduction was implemented for the rib and sternum cortical bone, rib cartilage, intercostal muscles and costovertebral ligaments in SOFT1-5.

TABLE I
MODELS, MODIFICATIONS AND LOAD CASES.

MODEL	ORGAN/TISSUE	MODIFICATION	ANALYSED DATA	LOAD CASES
HUMOS2LAB baseline model			rib strain profiles	A1 & C1-2
THUMS baseline model			rib cage deformation	B1-4 & D1
ATD-like modifications				
ATD1	HUMOS2LAB internal organs * lumbar muscles costovertebral joints	mass removed and 50% added to thoracic spine and 50% to ribcage mass removed and added to lumbar spine locked	rib strain profiles	A1 & C1-2
ATD2	THUMS rib cortical bone	elastic modulus increased by 50%	rib cage deformation	B1-4 & D1
ATD3	THUMS ribs rib cartilage	extended length comparable to THOR ribs reduced length proportionally	rib cage deformation	B1-4 & D1
ATD4	THUMS 1 st rib sternum	elastic modulus increased by 100% elastic modulus reduced by 90% for one row of elements at the level of the THOR bib between the upper and lower sternum	rib cage deformation	B1-4 & D1
ATD5	THUMS thoracic internal organs abdominal internal organs	density reduced by 80%, mass added to thoracic density reduced by 80%, mass added to lumbar	rib cage deformation	B1-4 & D1
ATD6	THUMS thoracic internal organs abdominal internal organs rib and sternum cortical bone costovertebral ligaments	mass removed and added to thoracic spine mass removed and added to lumbar spine elastic modulus increased by 150% elastic modulus increased by 900%	rib cage deformation	B1-4 & D1
ATD7	THUMS clavicle	horizontal orientation of superior surface	rib cage deformation	D1
Softer states				
SOFT1	THUMS rib cartilage	elastic modulus and yield stress decreased by 50%	rib cage deformation	B1-4 & D1
SOFT2	THUMS sternum cortical bone	elastic modulus and yield stress decreased by 50%	rib cage deformation	B1-4 & D1
SOFT3	THUMS intercostal muscles	elastic modulus decreased by 50%	rib cage deformation	B1-4 & D1
SOFT4	THUMS costovertebral ligaments	elastic modulus decreased by 50%	rib cage deformation	B1-4 & D1
SOFT5	THUMS rib cortical bone	elastic modulus and yield stress decreased by 50%	rib cage deformation	B1-4 & D1

* internal organs: lungs, heart, liver, spleen, stomach, kidney, thoracic soft tissues

Simulations

62 simulations were performed with either the baseline or the modified models in one of eight different load conditions according to Table I, described below:

Load case A1: Impactor test according to [29]. The models were loaded using a flat rigid disc, its diameter was 150 mm and the total impact mass was 23.4 kg. An impactor speed of 4.3 m/s was applied at 0°, see Figure 3.

Load case B1-B4: Table top tests with hub (B1), diagonal belt (B2), double diagonal belt (B3) and distributed loading (B4) according to [20]. The models were positioned on the table in a similar manner as described by [16] using a gravity loading simulation during 150 ms before applying restraint loading, resulting in the posture illustrated in Figure 4. The experimental rate at which the loading devices were pulled was 1 m/s. The simulations pulling rate was defined so that the chest deflection rate measured at the mid sternum position matched the experimental deflection rate.

Load case C1-C2: Frontal sled test with belt restraint according to [30]. The human body models were seated on a simplified mid-size car seat model. The models were either restrained by a 3-point belt (C1), where the shoulder belt was equipped with a 6 kN load limiter (Figure 5), or a combination of a 3-point belt and a fitted airbag (C2), where the shoulder belt was equipped with a 4 kN load limiter (Figure 6). Contact between the arms and the airbag was not taken into account. A knee bolster was present and the feet were fixed to the sled. A velocity change of 40 km/h was applied to the sled.

Load case D1: Frontal sled test with belt restraint according to [25] with a velocity change of 40 km/h, see Figure 7. The models were seated using gravity loading on a rigid seat and restrained with individual shoulder and lap belts firmly secured to the sled, a rigid footrest and rigid knee bolsters, similar to [31].



Fig. 3. HUMOS2LAB baseline model in the impactor test configuration (Load case A1).

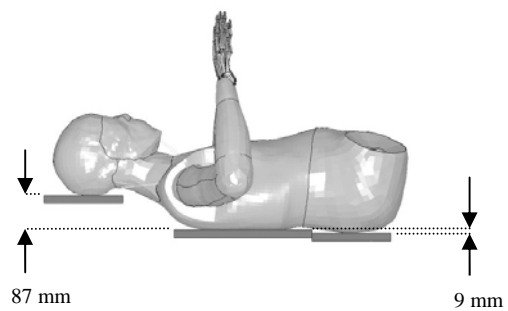


Fig. 4. THUMS baseline model in position for the table top load configurations (Load case B1-B4).



Fig. 5. HUMOS2LAB baseline model in the frontal sled test with belt (Load case C1).



Fig. 6. HUMOS2LAB baseline model in the frontal sled test with belt and airbag (Load case C2).



Fig. 7. THUMS baseline model in frontal sled test with belt (Load case D1).

Output

The modified models were compared to the baseline models with regards to rib strain (HUMOS2LAB), thoracic effective stiffness and deformation of the rib cage (THUMS). Rib strain in the HUMOS2LAB models were compared by means of four indicators:

- 1) Root Mean Square of strain (RMS), which reflects global strain level sustained by the rib, which is proportional to deformation energy absorbed by the rib in pure bending (Equation 1).

$$\varepsilon_{RMS}(t) = \sqrt{\frac{1}{((s1 - sn)_{left} + (sn - s1)_{right}) \left(\left(\int_{sn}^{s1} (\varepsilon(s,t))^2 ds \right)_{left} + \left(\int_{sn}^{s1} (\varepsilon(s,t))^2 ds \right)_{right} \right)}} \quad (1)$$

where $\varepsilon(s, t)$ is the strain at the curvilinear abscissa s as a function of time, $s1$ the curvilinear abscissa of the first shell element and sn is the curvilinear abscissa of the last shell element. The rib strain corresponds to the strain calculated in the shell elements on the external side of the ribs. The curvilinear abscissa s is equal to zero at the posterior end of each rib and reaches up to 100% at the anterior rib end. Positive values of s indicate ribs on the right side and negative values ribs on the left side.

- 2) Average normalised strain profile of each rib. The strain was normalised by RMS at each time step and then averaged in the time interval between 10% and 99% of maximum RMS. Low strains were excluded because of sensitivity to model noise and high strains just before maximum RMS were excluded since the strain at the location where the rib fracture occurred was dominating the rib strain profile. The maximum RMS of a rib corresponds to the peak value reached before the rib fracture occurs, predicted when the plastic strain of its shell elements exceeds 2.4% [28].
- 3) Normalised strain profile at the point where maximum RMS was reached.
- 4) Strain profile without normalization at the point where the maximum RMS was reached.

In THUMS and the modified versions, the rib cage deformation was output by tracking rib nodes A-E according to Figure 8. The effective stiffness is defined as the slope of the linear regression of the force-deflection curve, where the deflection is expressed as the mid-sternal (node A) compression relative to the initial chest depth at the eighth thoracic vertebra. The vertical coupling was calculated as the difference between the average deflection of nodes B and E and the average deflection of nodes C and D. The lateral coupling was defined as the difference between the deflections of nodes D and C.

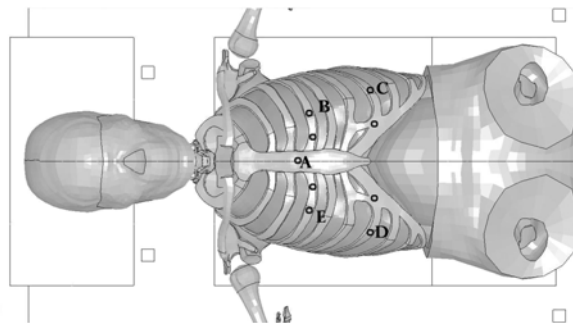


Fig. 8. Location of the tracked nodes used to study rib cage deformation with THUMS.

III. RESULTS

Strain profiles and RMS of ribs on their exterior side for the ATD1 and HUMOS2LAB baseline models are plotted in Appendix A; loaded with an impactor (A1, Figure A1) and simulated sled tests with belt (C1, Figure A2) and combined belt and airbag loading (C2, Figure A3). Exterior rib tensile strains were seen on the anterior portions and compressive strains were seen close to the posterior end. The strain profiles on the left and right sides were similar in the symmetric loading of the impactor. With belt only loading, the rib strain profiles were almost symmetrical for the first three ribs while all other rib levels had clearly asymmetrical loading, with pronounced tensile strains on the anterior right hand side portion. Comparing the ATD1 and baseline model, the strain profiles along the ribs were different in terms of strain levels, however, the strain distributions were similar for the modified and the baseline models for most of the rib levels. In general, the ATD1 had higher strain levels for the anterior tensile strains as well as the compressive strains close to the posterior end of the ribs.

The normalised effective stiffness is given in Table II for the modified models compared to the THUMS baseline model in the table top loading configurations. For the models that were made softer, the reduction in normalised effective stiffness ranged from 84% to unchanged. The most substantial reductions were seen in the hub load case (B1). The ATD-like versions of the THUMS produced both stiffer and weaker chest responses compared to the baseline model (Table II). The normalised sternal compression, lateral and vertical coupling are plotted in Figure 9 for the modified models compared to the THUMS baseline simulation. Under symmetrical loading, the chest deformations were such that the lateral coupling did not change when modified. This appears

to be the case also for the vertical coupling when the chest was loaded by the double diagonal belt (B3 in Figure 9). The sternal compression of the THUMS baseline simulation ranged between 30-36 mm in the table top loading conditions and 53 mm in the belted frontal sled loading.

TABLE II
THORACIC EFFECTIVE STIFFNESS FOR BASELINE AND MODIFIED MODELS FOR TABLE TOP LOADINGS.

MODEL	B1	B2	B3	B4
EFFECTIVE STIFFNESS [N/%]				
THUMS baseline	3670	11550	14040	16460
NORMALIZED EFFECTIVE STIFFNESS [%]				
THUMS baseline	100	100	100	100
SOFT1	95	98	99	99
SOFT2	96	97	100	100
SOFT3	88	93	92	89
SOFT4	99	98	100	99
SOFT5	84	92	91	93
ATD2	111	104	106	105
ATD3	110	104	101	98
ATD4	100	98	100	100
ATD5	92	94	93	90
ATD6	123	110	111	103

IV. DISCUSSION

An FE study comprising two different human body models was performed focusing on chest response and how model parameters influence the response in different load conditions relevant to modern restraint systems. Both models have previously been validated and the thorax response in particular, has been compared to numerous sets of experimental data. In the main part of this study, the THUMS model was used, focusing on the influence of ATD-like modification on the global thoracic deflection. The HUMOS2LAB model was used for an additional evaluation of rib strain profiles, focusing on the influence of internal thoracic organs. In fact, the HUMOS2LAB was not only validated in terms of its gross motion response, but also at deeper layers: its capability to predict rib strain profiles, the occurrence and the variation in location of rib fractures versus loading type and severity [27]-[28]. The validation level of the THUMS model did not allow such an approach. Based on these considerations, this study was performed comprising two baseline models.

Despite thorough validation, several numerical simplifications that will limit the results are presented herein. Furthermore, due to the modified models not representing real physiology it has not been possible to validate the modified models. Rather, the purpose of the models is to understand how anatomical ATD-like simplifications influence the biomechanics such as the rib fracture predictability and chest stiffness response, for example. The two models and the modifications were performed in different conditions, from the more traditional impactor-like loading to modern 3-point belt and airbag loading. The results are discussed in more detail below.

A limited sensitivity study was conducted with THUMS by reducing material parameters for the cortical bone in the ribs, sternum, cartilage, intercostal muscles, and the costovertebral ligaments as well as increasing the stiffness of the rib cortical bone. The change from the baseline values was 50%. This substantial difference was considered relevant in order to illustrate the influence of each tissue on the global stiffness response of the chest. A similar approach was adopted by [15] in a study comprising an early version of the THUMS model.

The material properties of the rib cortical bone and intercostal muscles had the most influence on the chest deflections and stiffness. It is interesting to note that the sternum had a limited influence in all the table top loading configurations, while it increased the chest compression in a frontal sled test by 9%. Hence, the properties of the sternum seem to be more important when the chest is loaded by the inertia of the internal organs. This may also hold true for the rib cortical bone, where the normalised sternal deflections were greater in the frontal sled test, compared to the table top loading cases. Minor effects on chest displacement and stiffness were seen by changing the properties of the costovertebral ligaments and rib cartilage.

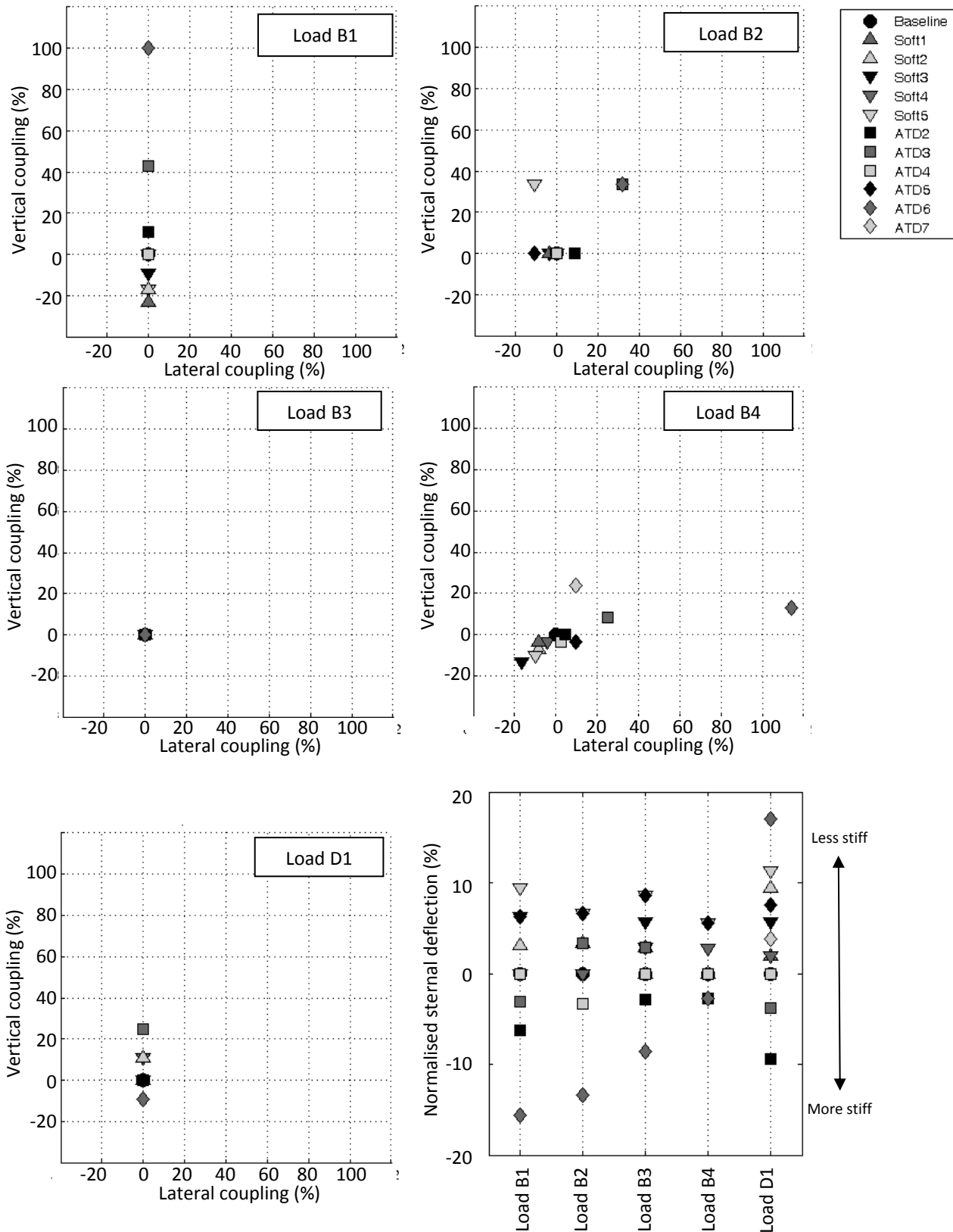


Fig. 9. Vertical versus lateral coupling and normalised sternal compression for the modified models compared to the THUMS baseline model.

The influence of the material properties on the lateral and vertical coupling was most substantial in diagonal belt loading. Overall, reducing material stiffness reduced the chest coupling in both vertical and lateral directions for the frontal sled test, even though such modifications had negligible effects on the coupling in the table top loading. The rib cortical bone stiffness affected the coupling of the chest loaded by a diagonal belt differently for the table top and frontal sled test conditions; a decrease of the cortical bone stiffness increased the coupling in the table top loading and decreased the coupling in the frontal sled test. However, the vertical coupling in the table top test with diagonal belt loading should be treated with caution as the highest value, 1.3, corresponded to only a 1 mm change in peak difference between the nodes. It seems that the model was most sensitive with respect to chest coupling in sled test loading. The stiffness of the intercostal muscles, ribs and sternum has the greatest influence on coupling.

A number of modifications representing features of ATDs were performed to evaluate what biomechanical consequences may result from these design choices. It became apparent that splitting the sternum between the first and second rib levels, similar to the dummy bib, did not influence the chest compression, lateral or vertical coupling. It can also be noted that design changes to the clavicle had a small effect on the deformation pattern; modifying the clavicle orientation appears to shield the upper right part of the torso when loaded with a 3-point belt. All other modifications altered the effective stiffness by at least 10%. Of the different simulated conditions, increasing rib stiffness and length had the most pronounced effect on the stiffness in hub loading. Reducing density of the internal organs and transferring the removed mass to the spine increased the chest deflection for all load cases. This is easily explained by a decrease in the inertia working against chest compression. Shifting the internal organ mass to other structures does not change the characteristics of the strain profile very much. However, for shoulder belt loading configurations, the modifications resulted in a strain amplitude decrease on the side without belt loading of the lower ribs (7th, 8th, 9th and 10th ribs), but an increase in strain on the belt loading side, in particular near to the spine. This means that the action of belt loading is locally accentuated with internal organ mass transfer. However, such modification to the strain profile does not modify the maximum strain locations and therefore does not constitute a fundamental change in predicted fracture location. The lack of internal organ mass in an ATD may be compensated by an increase in rib stiffness. However, these results show that, for a model where the mass of the internal organs was transferred to the spine and the stiffness of the ribs was increased, the chest response will be significantly different if loaded in a table top configuration compared to a sled test loading. In this study, the sternal compression decreased by up to 16% in the table top tests and increased by 17% for a sled test.

ATDs do not have any internal organs in the thorax cavity. The lack of internal organ representation is primarily compensated by adding mass to the spine, ribs and sternum. In this study, simulation comprising two models modified with ATD-like simplifications illustrated that for asymmetric loading, the rib strain profile was accentuated by local strain concentrations and the differential chest deflections were decreased. It may be possible to achieve biofidelic mid chest compression in an ATD in a sled test by increasing the rib stiffness until the response is sufficient. However, our simulations indicate that then the lateral and vertical coupling will increase to an extent where it will become difficult to assess the regional differences in chest compression. Therefore, it may be problematic to use injury criteria including differential deflections which imply that an ATD designed to distinguish between different modern restraints, may require a representation of the internal organs, and the ribs should not be made too stiff. Internal organs could possibly be represented by providing some load path between the spine box and the sternum, for example linear dampers/springs between the spine and the sternum. However, if the differential deflection is of less importance for safety restraint development, it may be reasonable to compensate for the lack of internal organs by adding mass and stiffness to the rib cage.

V. CONCLUSIONS

Removing internal organs result in global stiffness decrease of the thorax. However, it does not change the main features of the rib strain profile. If the stiffness decrease of the thorax in an ATD without internal organ representation is compensated by using stiffer rib materials, the lateral and vertical coupling will increase. Therefore, there is a compromise between stiffness and mass representation in order to measure biofidelic differential chest deflections.

VI. ACKNOWLEDGEMENT

This study was funded by the European Commission Seventh Framework Programme 7, Transport, SST.2007.4.1.2: Human physical and behavioural components, grant number: 218516. This work has partly been carried out in the environment at SAFER - Vehicle and Traffic Safety Centre at Chalmers, Sweden.

VII. REFERENCES

- [1] Frontal Impact Dummy, GROWTH Project GRD1-1999-10559 "FID", Performance of existing dummies, *WP4 Final Summary Report*, Technical document compiled by TRL Limited, UK, 2003.
- [2] PRISM R9/R10 Report on Recommended Functional Requirements Including Modelling and Testing for Smart Restraint Systems. PRISM Report No: 0415024 (contr. GRD2-2001-50109), 2006.
- [3] Cuerden R, Damm R, Pastor C, Barberis D, Richards D, Edwards M, An estimation of the costs and benefits of improved car to car compatibility on a national and European scale. VC-Compat Growth project GRD2-2001-50083, Deliverable 24, 2006.
- [4] Shams T, Rangarajan N, McDonald J, Wang Y, Platten G, Spade C, Pope P, Haffner M, Development of THOR NT: Enhancement of THOR Alfa – the NHTSA Advanced Frontal Dummy. Paper No. 05-0455, *Proc. of the 19th ESV Conference*, Washington DC, US, 2005.
- [5] Kent R, Patrie J, Benson N, The Hybrid III dummy as a discriminator of injurious and non-injurious restraint loading. *Annual Proceedings/Association for the Advancement of Automotive Medicine* 47:51-75, 2003.
- [6] Forman J, Kent R, Ali T, Crandall J, Boström O, Håland Y, Biomechanical Considerations for the Optimization of an Advanced Restraint System: Assessing the Benefit of a Second Shoulder Belt, *Proc. of the IRCOBI Conference*, Prague, Czech Republic, pages 337-353, 2005.
- [7] Langwieder K, Fildes B, Ernvall T, Cameron M, SARAC – Safety rating system based on real-world crashes for supplementation of New Car Assessment programs. *Proc. of the 18th International Technical Conference on the Enhanced Safety of Vehicles*; Nagoya. Paper number 175, 2003.
- [8] Hallquist, J. O. LS-DYNA Keyword user's manual. Version 970, Livermore Software Technology Corporation, Livermore, US, 2006.
- [9] Radioss Starter Version 4.4 Block Format, Revision 2.0, Mecalog, France, April 30, 2004.
- [10] User's Guide of Computational Human Model THUMS - AM50 Occupant Model: Version 3.0-080225. Toyota Motor Corporation Toyota Central Labs Inc, Japan, 2008.
- [11] Vezin P, Verriest J-P, Development of a set of numerical human model for safety. *Proc. of the 19th Int. Tech. Conf. on the Enhanced Safety of Vehicles*, Paper Number 05-0163, 2005.
- [12] Oshita F, Omori K, Nakahira Y, Miki K, Development of a Finite Element Model of the Human Body, *7th International LS-Dyna Users' Conference*, Detroit, US, 2002.
- [13] Iwamoto M, Kisanuki Y, Watanabe I, Furuusu K, Miki K, Hasegawa J, Development of a Finite Element Model of the Total Human Model for Safety (THUMS) and Application to Injury Reconstruction, *Proc. of the IRCOBI Conference*, Munich, Germany, pages 17-36, 2002.
- [14] Furuusu K, Watanabe I, Kato C, Miki K, Hasegawa J, Fundamental study of side impact analysis using the finite element model of the human thorax, *JSAE Review*, 22(2): 195-199, 2001.
- [15] Kimpara H, Iwamoto M, Watanabe I, Miki K, Lee JB, Yang KH, King AI, Effect of assumed stiffness and mass density on the impact response of the human chest using a three-dimensional FE model of the human body, *Journal of Biomechanical Engineering-Transactions of the ASME*, 128(5): 772-776, 2006.
- [16] Murakami D, Kobayashi S, Torigaki T, Kent R, Finite element analysis of hard and soft tissue contributions to thoracic response: sensitivity analysis of fluctuations in boundary conditions, *Stapp Car Crash Journal*, 50: 169-89, 2006.
- [17] Pipkorn B, Mroz K, Validation of a Human Body Model for Frontal Crash and its Use for Chest Injury Prediction, *SAE Int. J. Passeng. Cars - Mech. Syst.* 1(1):1094-1117, 2009.
- [18] Mroz K, Boström O, Pipkorn B, Wismans J, Brolin K, Comparison of HYBRID III and Human Body Models in Evaluating Thoracic Response for various Seat Belt and Airbag Loading Conditions, *Proc. of the IRCOBI Conference*, Hanover, Germany, pages 293-296, 2010.
- [19] Ruan J, El-Jawahri R, Chai L, Barbat S, Prasad P, Prediction and analysis of human thoracic impact responses and injuries in cadaver impacts using a full human body finite element model, *Stapp Car Crash Journal*, 47: 299-321, 2003.
- [20] Kent R, Lessley D, Sherwood C, Thoracic response to dynamic, non-impact loading from a hub, distributed belt, diagonal belt, and double diagonal belts, *Stapp Car Crash Journal*, 48: 495-519, 2004.

- [21]Mendoza-Vazquez M, Davidsson J, Brolin K, Influence of rib boundary condition on rib response: a comparison between single rib and complete body tests using a Human Body Model, draft manuscript, 2012.
- [22]GESAC, Biomechanical response requirements of the THOR NHTSA advanced frontal dummy (Revision 2005.1), GESAC-05-03, 2005.
- [23]Kent R, Sherwood C, Lessley D, Overby B, Matsuoka F, Age Related Changes in the Effective Stiffness of the Human Thorax Using Four Loading Conditions. *Proc. of the IRCOBI Conference*, Lisbon, Portugal, pages 249-264, 2003.
- [24]Kent R, Murakami D, Kobayashi S, Frontal thoracic response to dynamic loading: the role of superficial tissues, viscera and the ribcage. *Proc. of the IRCOBI Conference*, Prague, Czech Republic, pages 355-365, 2005.
- [25]Shaw G, Parent D, Purtsezov S, Lessley D, Crandall J, Kent R, Guillemot H, Ridella S, Takhounts E, Martin P, Impact response of restrained PMHS in frontal sled tests: skeletal deformation patterns under seat belt loading, *Stapp Car Crash Journal*, 53: 1-48, 2009.
- [26]Robin, HUMOS: Human model for safety - A joint effort towards the development of refined human-like car occupant models. *Proc. of the 17th Int. Tech. Conf. on the Enhanced Safety of Vehicles*, Paper Number 297, 2001.
- [27]Song E, Trosseille X, Baudrit P, Evaluation of Thoracic Deflection as an Injury Criterion for Side Impact Using a Finite Elements Thorax Model. *Stapp Car Crash Journal*, 53: 155-191, 2009.
- [28]Song E, Lecuyer E, Trosseille X, Development of Injury Criteria for Frontal Impact Using a Human Body FE Model. *Proc. of the 22nd Int. Tech. Conf. on the Enhanced Safety of Vehicles*, Washington D.C., paper no 11-0330-O, 2011.
- [29]Kroell, C., Schneider, D., Nahum, A, Impact Tolerance of The Human Thorax II. *Proc. of the 18th Stapp Car Crash Conference*, pp. 84-134. Society of Automotive Engineers, Warrendale, PA, 1974.
- [30]Petitjean A, Lebarbé M, Potier P, Trosseille X, Lassau J-P, Laboratory reconstructions of real world frontal crash configurations using the H-III and THOR dummies and PMHS. *Stapp Car Crash Journal* 46: 27-54, 2002.
- [31]Untaroiu CD, Lim JY, Shin J, Evaluation of a thor dummy rigid-body model in frontal crash environment using objective rating techniques, *Biomed Sci Instrum*, 45: 95-100, 2009.

VIII. Appendix A

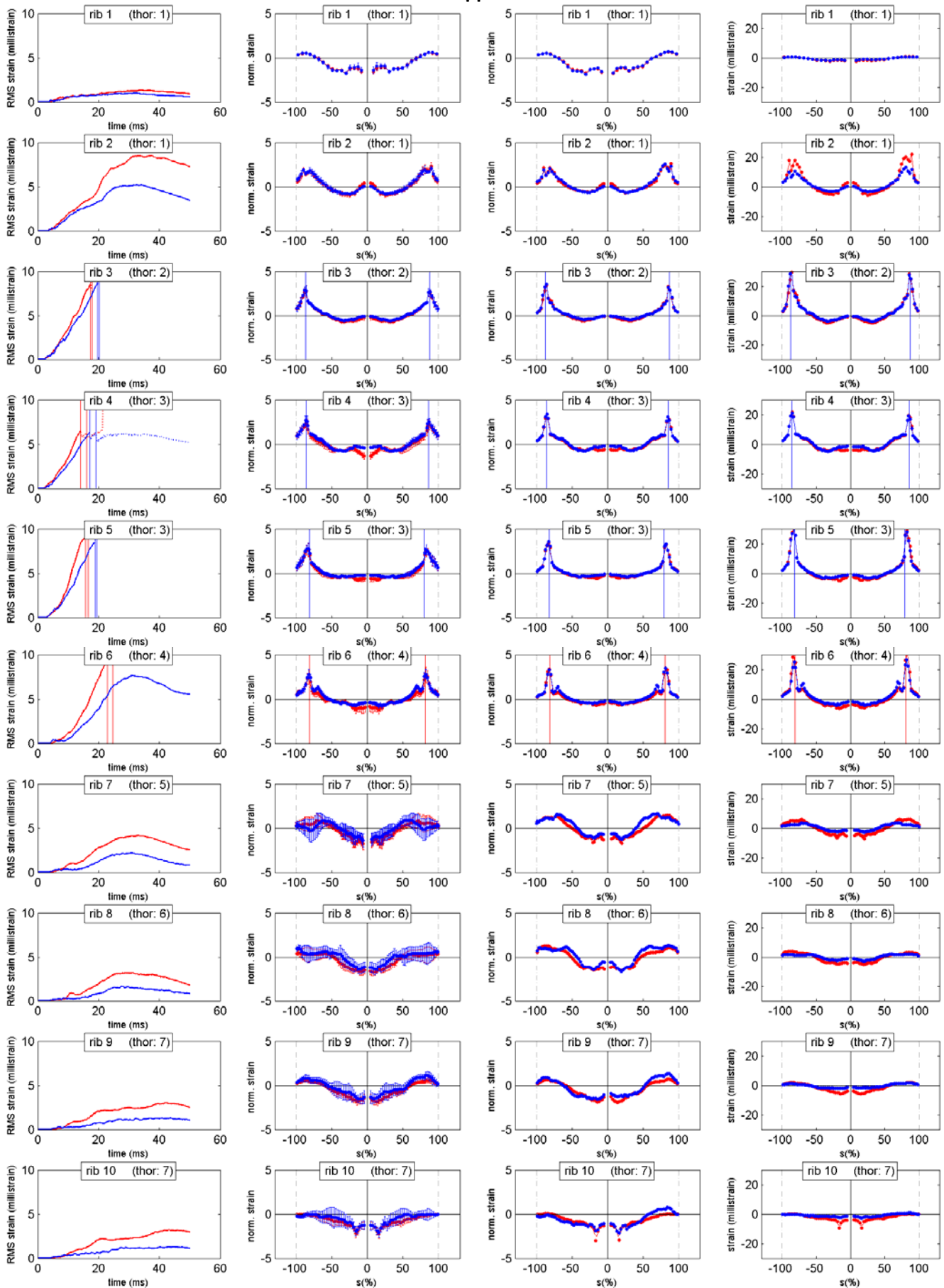


Figure A1. Comparison of rib strain by means of four indicators for the frontal impactor test A1 between the HUMOS2LAB baseline model (blue) and ATD1 (red): RMS (Column 1), average normalised strain profile (Column 2), normalised strain profile at the RMS peak time (Column 3) and strain profile without normalisation at the RMS peak time (Column 4).

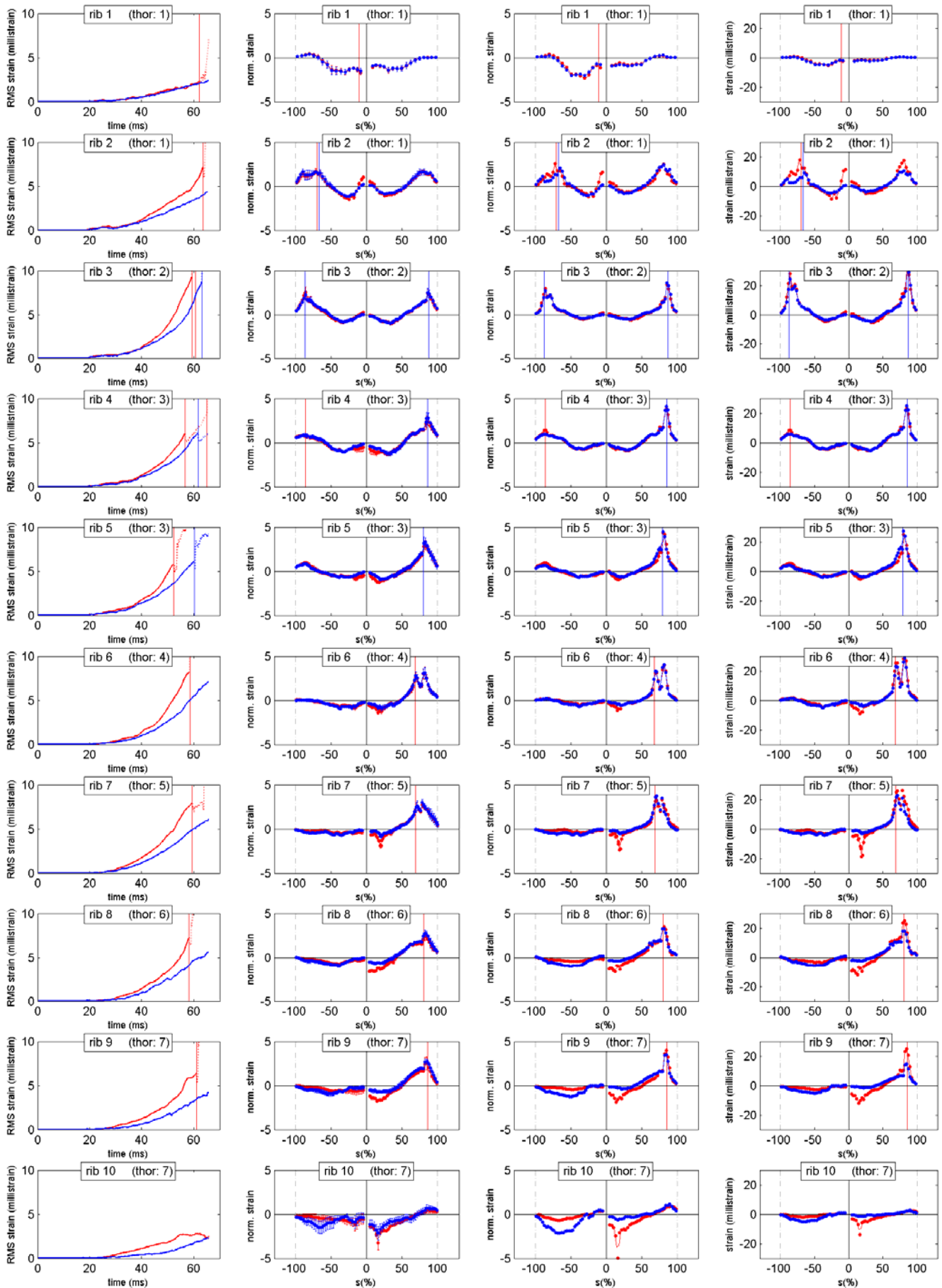


Figure A2. Comparison of rib strain by means of four indicators for the frontal belt only sled test C1 between the HUMOS2LAB baseline model (blue) and ATD1 (red): RMS (Column 1), average normalised strain profile (Column 2), normalised strain profile at the RMS peak time (Column 3) and strain profile without normalisation at the RMS peak time (Column 4). For RMS curves, the portions beyond rib fracture were plotted in dotted lines.

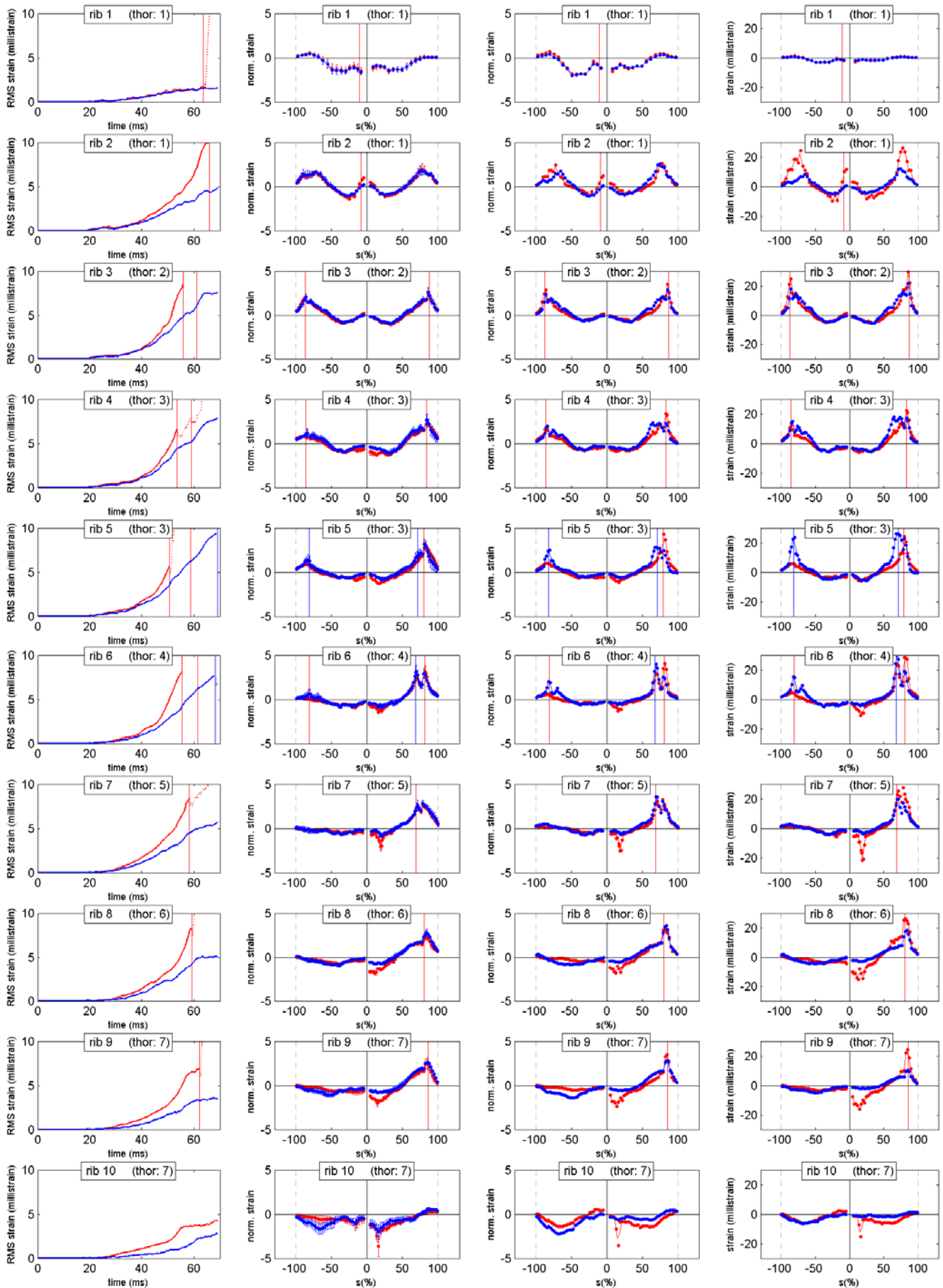


Figure A3. Comparison of rib strain by means of four indicators for the frontal sled test with combined belt and airbag loading C2 between the HUMOS2LAB baseline model (blue) and ATD1 (red): RMS (Column 1), average normalised strain profile (Column 2), normalised strain profile at the RMS peak time (Column 3) and strain profile without normalisation at the RMS peak time (Column 4). For RMS curves, the portions beyond rib fracture were plotted in dotted lines.